AD-A117 315 ARMY NIGHT VISION LAB FORT BELVOIR VA F/G 20/3
ELECTRICAL PROPERTIES OF HEATED DIELECTRICS.(U)
JUN 82 E J SHARP, L E GARN

UNCLASSIFIED NL

END
DATE FILMED
8-82
DTIC

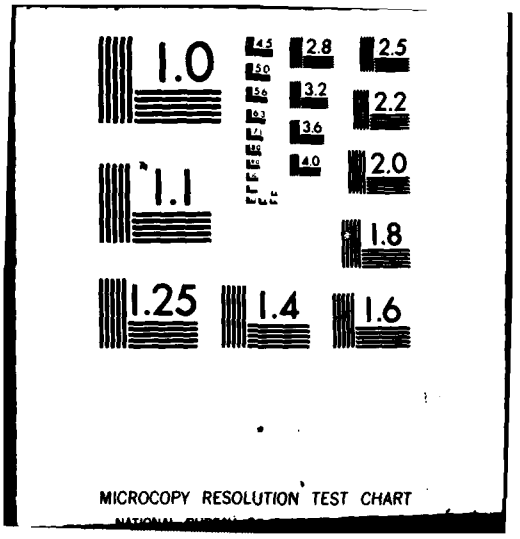
1.0
1.1
1.25
1.4
1.6
1.8
2.0
2.2
2.5
2.8
3.2
3.6
4.0
4.5
5.0
5.6
6.3
7.1
8.0
9.0
MICROCOPY RESOLUTION TEST CHART

(1)

ELECTRICAL PROPERTIES OF HEATED DIELECTRICS (U)

*EDWARD J. SHARP, DR.
LYNN E. GARN, DR.
NIGHT VISION AND ELECTRO-OPTICS LABORATORY
FORT BELVOIR, VIRGINIA 22060

INTRODUCTION

For the past decade there has been a great deal of work devoted to understanding the pyroelectric and piezoelectric mechanisms in several of the high polymers, most notably in the material poly(vinylidene fluoride), PVF_2. At the present time PVF_2 has the highest piezo-pyroelectric response among polymeric materials. Since the early work on the pyroelectric properties of PVF_2 by Nakamura and Wada (1) and Bergman et al (2), considerable effort has been expended in attempts to improve the pyroelectric response of this polymer for numerous practical applications including reflectivity measurements (3), a photocopy process (4), infrared radiation detection (5),(6), thermal imaging with a pyroelectric vidicon (7),(8), intrusion and fire detection (9), and non-linear optical devices (2). In spite of this intense activity the nature of the mechanism (or mechanisms) of pyroelectricity in PVF_2 is not fully understood (10),(11). To a large extent much of the confusion surrounding the understanding of the electrical behavior of this important material is due to ambiguous results associated with the interpretation of different measurement techniques used to explore its properties.

Several techniques have been used in the past to accurately determine the pyroelectric properties of dielectric materials (4),(12),(13),(14). Some of these techniques have been reviewed recently regarding their usefulness in the characterization of pyroelectric materials intended for use as infrared radiation detectors or as targets in a pyroelectric vidicon (PEV) (8). As radiation detectors, pyroelectric materials must exhibit a current response that is completely reversible and reproducible when subjected to small temperature changes.

There are numerous materials which exhibit a large non-pyroelectric current response (non-reversible) when they are heated (15). There are also many materials which are capable of exhibiting both non-pyroelectric and pyroelectric responses simultaneously when they are heated. Since only the reversible pyroelectric current contributes to infrared response, it is obvious that any technique used to evaluate such materials for use as

infrared radiation detectors must provide the capability for distinguishing the current contributions associated with pyroelectric behavior and those associated with non-pyroelectric behavior and to permit the determination of their individual magnitudes.

Typically PVF_2 film is only weakly pyroelectric in the as received condition. When PVF_2 is subjected to an applied electric field (poling), significant pyroelectric response can be generated in the film and this response may be further enhanced or degraded by additional or simultaneous thermal and mechanical treatments (stretching). A recent review article on PVF_2 by Das-Gupta (16) discusses these poling techniques and their subsequent effects on the structure, pyroelectric behavior, and the possible models to explain this behavior.

It has been reported (8),(17) that the first thermal cycle of a poled PVF_2 sample will yield a predominantly non-pyroelectric current (thermally stimulated current or conductivity, TSC) (15) as a function of temperature and that the second and subsequent thermal cycles yield a reversible pyroelectric current (4). The shape of the first thermal cycle current curve depends upon the poling procedure (18). Here we describe a new method which allows the analysis and evaluation of electric currents such as pyroelectric currents and thermally stimulated currents arising from heated dielectric materials. This method can be applied to materials that exhibit only pyroelectric currents, materials that exhibit only non-pyroelectric currents, or materials that exhibit a combination of the two types of currents. Pyroelectric current is directly proportional to the derivative of temperature with respect to time. Non-pyroelectric current, in general, is either constant or within small temperature intervals nearly proportional to the temperature. These assumptions have been verified (19),(20) mathematically in certain temperature and frequency ranges and experimentally for a number of different dielectric materials, several of which will be discussed here. Poly(vinylidene fluoride) has been selected as one of the materials since it is an important material from an applications point of view. It also lends itself well to demonstrating the strength and validity of the following treatment and measurements.

THEORY

For the present we assume that non-pyroelectric currents can be represented by

$$i_g = i_o + RT \,, \qquad [1]$$

where i_o is a constant, non-pyroelectric, temperature independent current. The term RT is also non-pyroelectric, but it increases linearly with temperature T; R, being a temperature coefficient. It

has been shown previously (20) that within small temperature intervals TSC can be approximated by this form. Equation [1] is used because it is general and applies to any non-pyroelectric current that may be present.

The pyroelectric current can be written as (12),(14)

$$i_\pi = pA\frac{dT}{dt} , \qquad [2]$$

where p is the pyroelectric coefficient A, the sample area and dT/dt the time derivative of the temperature.

In a material where both currents are present the total current can be written as

$$i_T = i_o + RT + pA\frac{dT}{dt} . \qquad [3]$$

In typical measurements of TSC and pyroelectric current, the sample temperature is $T_o + bt$, where T_o denotes the initial absolute temperature of the sample and bt is the temperature change introduced when the sample is heated at a constant rate b for a time t (14),(21),(22). If, in addition to this normal method of heating, a small sinusoidal temperature component of amplitude T_1 and angular frequency ω is imposed on the sample, the temperature becomes

$$T = T_o + bt + T_1\sin(\omega t) . \qquad [4]$$

The total current from the sample under these heating conditions can now be written as a sum of an ac-current and a dc-current as

$$i_T = [i_o + R(T_o + bt) + pAb] + [RT_1\sin(\omega t) + pAT_1\omega\cos(\omega t)] . \qquad [5]$$

For sufficiently large frequencies the term Rbt is nearly constant during the period of a heat wave and is therefore included in the dc-current term. It is important to note that the term $RT_1\sin(\omega t)$, which is in phase with the sinusoidal component of temperature, comes from the non-pyroelectric part of Eq. [3]. On the other hand, the term $PAT_1\omega\cos(\omega t)$ comes from the pyroelectric component of Eq. [3] and the resulting current precedes the sinusoidal temperature wave by 90°. Thus ac-components of non-pyroelectric currents are in phase with the temperatur whereas ac-components of pyroelectric currents precede the temperature by 90°. The ac portion of the current given by Eq. [5] can be written as

$$i_{ac} = i_1\sin(\omega t + \theta) , \qquad [6]$$

where

$$i_1 = (i_n^2 + i_p^2)^{1/2} , \quad [7]$$

$$i_n = RT_1 , \quad [8]$$

$$i_p = pAT_1\omega , \quad [9]$$

$$\theta = \tan^{-1}(i_p/i_n) = \tan^{-1}(pA\omega/R) . \quad [10]$$

The amplitudes of the non-pyroelectric and pyroelectric currents are given by i_n and i_p respectively. The amplitude of the ac-current i_1 therefore depends upon the amplitude of both the pyroelectric current and the non-pyroelectric current. An examination of the amplitude of the ac-component i_1 is not sufficient to determine if the current is pyroelectric or non-pyroelectric. The phase difference θ between the temperature and current waves must be determined to establish which type of current is present. For example, in a purely pyroelectric material i_n will be zero and $\theta = 90^o$, and for a material with no pyroelectric response i_p will be zero and $\theta = 0^o$. When a material exhibits both types of currents the extrema of the ac-current precede the extrema of the temperature by a phase angle somewhere between 0^o and 90^o. Thus if we measure the phase of the ac-current with respect to the temperature wave, we can determine if the current is pyroelectric or non-pyroelectric and we can use Eq. [7] and [10] to compute the fraction of current associated with each effect. These components are:

$$i_p = i_1 \sin(\theta) , \quad [11]$$

$$i_n = i_1 \cos(\theta) . \quad [12]$$

It has been shown that the TSC arising from numerous relaxation processes has the following time and temperature dependence (15),(21),(22).

$$i_b = C \exp\left[\frac{-E}{kT} - B\int_0^t \exp\left(\frac{-E}{kT}\right) dt\right] . \quad [13]$$

where the constants C and B depend on the origin of the TSC. This relation assumes a single relaxation time of the form $\tau = \tau_o \exp[E/kT]$ where τ_o is a constant, E is an activation energy, and k is Boltzmann's

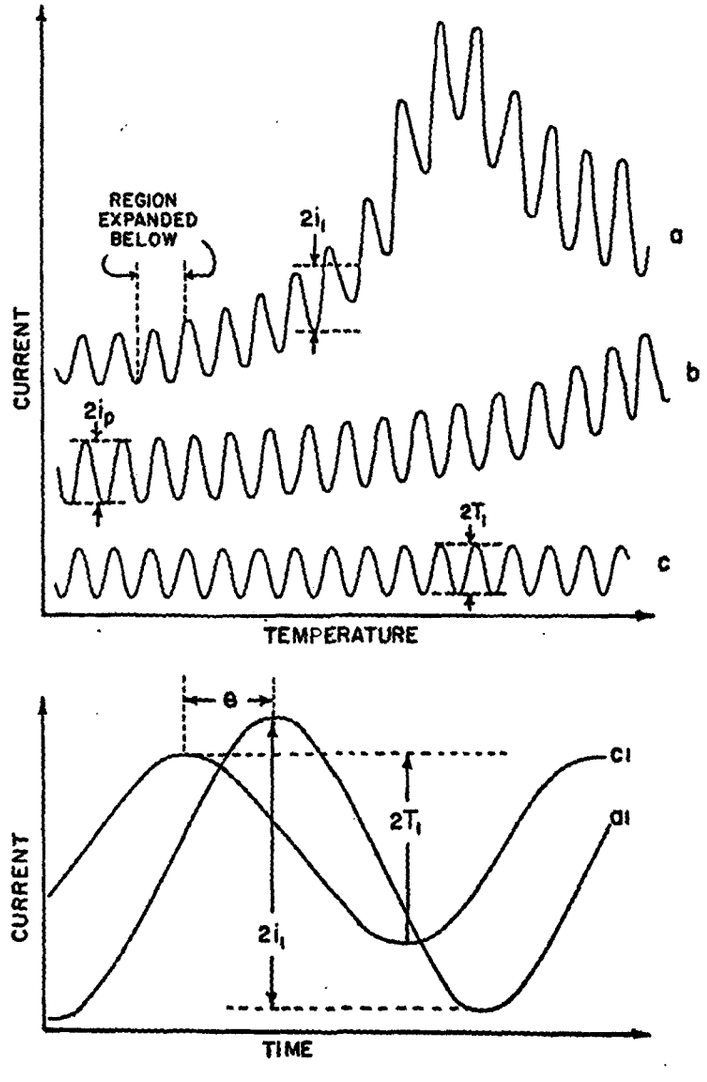

Figure 1. Sketch of actual data for a pyroelectric material such as PVF_2. A small section of the current versus temperature data is expanded in the lower set of curves to illustrate the observed phase shift, θ. Curve (a) represents the current arising from a first thermal cycle, curve (b) is the current arising from subsequent theral cycles, and curve (c) is the ac-temperature wave.

constant. This assumption is consistent with our observations of TSC curves of PVF_2 samples rested equal lengths of time (18). There is some temperature T_m at which maximum TSC occurs for a sample heated at a constant rate b, ($T = T_o + bt$) determined by maximizing Eq. [13] with respect to t. The value of T_m depends strongly upon the rest time after poling and in general the TSC decreases sharply for $T > T_m$ (18).

It has been previously shown (20) that within small temperature intervals the TSC given by Eq. [13] is a linear function of temperature for a constant heating rate of the form $T = T_o + bt$. For temperatures of the form given by Eq. [4] i_b is non-pyroelectric and can be represented by Eq. [1]. Where the period of the sinusoidal temperature wave and the heating rate can be chosen such that i_o and R change very little during several periods of the heat wave (20). The value of R is then expressed as:

$$R = \frac{i_b E}{k(T_o + bt)^2} \quad . \qquad [14]$$

It is useful to examine the influence of the temperature dependence of R on the magnitude and phase of the ac-current. We can rewrite the expression for the amplitude of the ac-component i_1 in terms of the pyroelectric and non-pyroelectric current amplitudes given by Eqs. [8] and [9].

$$i_1 = \left[\left(\frac{i_b E T_1}{k(T_o + bt)^2}\right)^2 + (pA\omega T_1)^2\right]^{1/2} , \qquad [15]$$

where R has been written in the form given by Eq. [14]. Since i_b has the characteristic TSC dependence on temperature, the non-pyroelectric amplitude and therefore the ac-component i_1 will increase as i_b increases to its maximum at T_m. As the temperature is increased beyond T_m, i_b decreases to zero and the first term in Eq. [15] vanishes and i_1 is then equal to the amplitude of the pyroelectric current. The change in i_b with temperature does not influence i_p but it does influence the phase angle. Since θ decreases as R increases, θ will reach a minimum when i_b is a maximum at the temperature T_m. The amplitude and phase of the ac-current, i_1, and θ, can be measured directly and compared with computed values.

To better understand this procedure, Fig. 1 is presented. It represents an actual display of data taken on a sample that exhibits both TSC and pyroelectric response such as a PVF_2 sample might have. This figure is used to identify the various parameters associated with the theory and to demonstrate how to extract the information necessary to

apply the theory from a typical sample of recorded data.

When a sample is thermally cycled for the first time curves (a) and (c) are recorded concurrently. Curve (a) is the total current, pyroelectric and non-pyroelectric, released from the sample as it is heated under the conditions given by Eq. [4]. Curve (c) is a recording of only the sinusoidal portion of the applied temperature, $T_1 \sin(\omega t)$, which oscillates about (T_o+bt). For each subsequent thermal cycle the current, curve (b), and a new curve (c) are recorded so that phase measurements can be made. It is important to note that curve (a) as shown in Fig. 1 is representative of those obtained on PVF_2. In materials which exhibit only pyroelectric response curves (a) and (b) will be identical. At selected temperatures (T_o+bt, see Eq. [4]) throughout the thermal cycle, usually every 10°C, new curves (c1) and (a1) are recorded to graphically magnify the phase difference betweeen them.

The analysis of data is simplified by noting that A and k are constants, ω and T_1 are fixed by the temperature wave period, and the quantity (T_o+bt) is just the measurement temperature at some time t during the thermal cycle. The values of the three quantities remaining in the expression for the ac-current amplitude, i_b, E, and p along with the phase difference can be extracted from the data as follows: the pyroelectric coefficient, p, can be estimated using second run current dc-values (18). This, together with the values of A, T_1, and ω, provides a computed value for the amplitude of the ac-pyroelectric current component $pAT_1\omega$. If the dc-component of the curve (a) is measured and the dc-component of curve (b) is subtracted off (18), the resulting current i_b can be subjected to the usual (21), (22) TSC analysis and a determination of the activation energy can be made. The amplitude of the non-pyroelectric ac-current can be computed from Eq. [8]. The values i_n and i_p can now be used to compute i_1 and θ which may then be compared with the measured values.

EXPERIMENTAL RESULTS

We have examined two ferroelectric materials in the temperature range 0°C to 80°C: triglycine sulfate (TGS), $(NH_2CH_2COOH)_3 \cdot H_2SO_4$, and lithium tantalate, $LiTaO_3$. Samples of each material were prepared from 50 m thick wafers having circular nichrome electrodes deposited on both sides so that they formed capacitors with an area of $0.6cm^2$. Fine wire leads were silver-epoxied to non-overlapping tabs extending from the circular electrodes and the samples were poled at room temperature with dc-electric fields of $10^3 - 10^4$ V/cm for both materials.

TGS exhibits Curie behavior in this temperature range at ~ 49°C but $LiTaO_3$ does not since it is a high-temperature ferroelectric with a Curie temperature $T_c \approx 618$°C (23),(24). Figure 2 shows the measured ac- and dc-components of pyroelectric current for lithium tantalate as a function of temperature from 0°C to 80°C for 5, 10, 20, 50, 100, and

STAMP Security Classification here

SHARP AND GARN

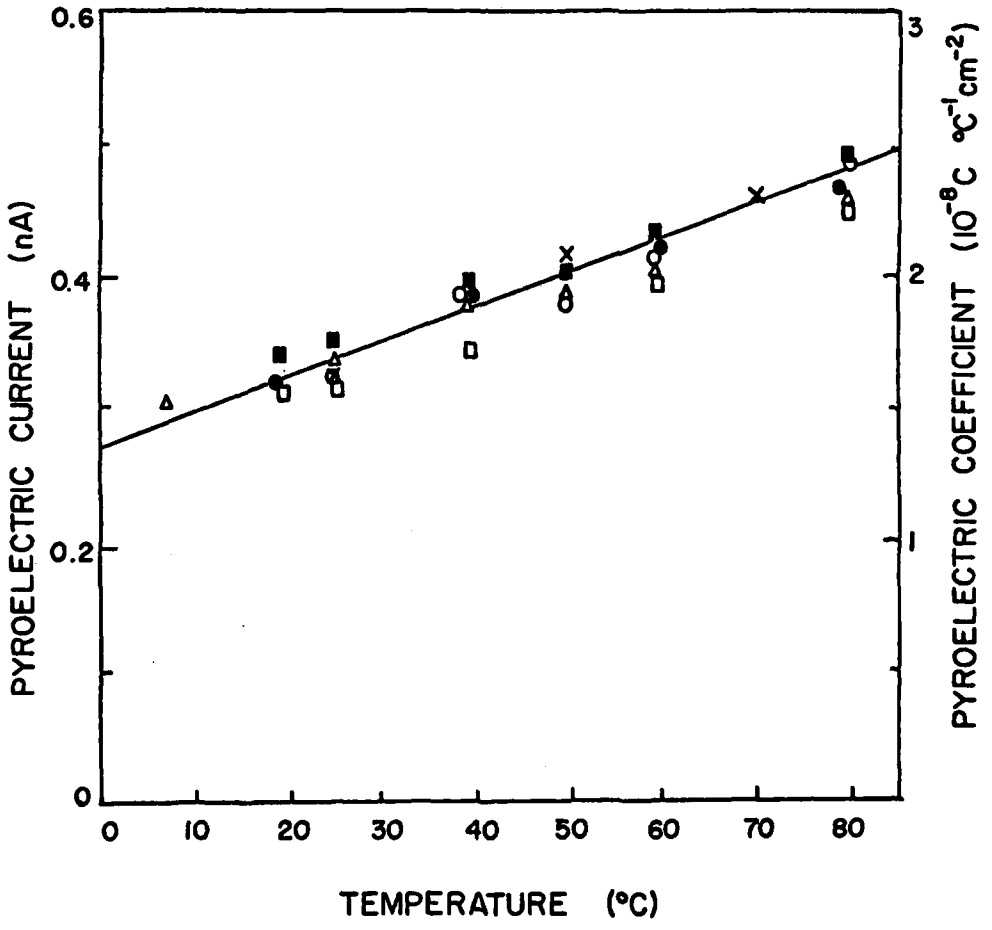

Figure 2. Pyroelectric current as a function of temperature for $LiTaO_3$. The values of the pyroelectric coefficients associated with these currents are also shown. Here the straight line is the measured dc-value of the pyroelectric current and the ac-values are for different temperature wave periods as: (5 sec-X), (10 sec-■), (20 sec-□), (50 sec-△), (100 sec-●), and (200 sec-○).

STAMP Security Classification here

200 sec temperature wave periods. The value of the pyroelectric coefficient for $LiTaO_3$ at 25°C is in agreement with the values reported by other workers (14),(24),(25), 1.76×10^{-8} C/cm^2 to 1.9×10^{-8} C/cm^2 °C.

The pyroelectric coefficients for TGS obtained from the measured ac and dc-components of the current are compared in Fig. 3. The value of the pyroelectric coefficient, $p = 3 \times 10^{-8}$ C/cm^2 °C obtained at 23°C agrees well with the values reported by others, (25),(26), 2.8×10^{-8} C/cm^2 °C and $2\text{-}3.5 \times 10^{-8}$ C/cm^2 °C. The markedly different pyroelectric response curves for TGS and $LiTaO_3$ shown in Figs. 2 and 3 stem from the fact that TGS exhibits Curie behavior in the measurement temperature range. Even though the measured pyroelectric response of TGS varies nearly two orders of magnitude and $LiTaO_3$ varies only slightly, there is good agreement between the ac and dc-current components for both materials.

The phase difference for these two materials is determined graphically as described earlier and these values are shown in Fig. 4 from 0°C to 80°C. The $\pi/2$ phase shifts at all temperatures indicate that i_1 has no non-pyroelectric ac-component and thereby confirms that the materials are purely pyroelectric.

Hundreds of PVF_2 samples were prepared from 6 m thick biaxially oriented film and electroded to form capacitors in the same manner as the ferroelectric materials. These samples were then poled at relatively high fields, 1.3×10^6 V/cm, at room temperature. This procedure assured that the samples were well poled as described by Day et al (27).

The currents from these samples were recorded as a function of temperature from 0°C to 80°C at a 2°/min heating rate in the presence of a small low-frequency sinusoidal temperature wave. Each specimen was measured several times and data similar to that depicted in Fig. 1 was obtained for each sample. Pyroelectric coefficients obtained at room temperature of 1×10^{-9} C/cm^2 C° are in good agreement with those of a number of other workers for similarily poled samples (27),(28). Following the analysis procedure outlined earlier, the phase shifts for the first thermal cycles of identically poled and rested samples are shown in Fig. 5 for temperature wave periods of 5, 20, 50, and 100 seconds.

Note that in these curves the position of the maximum phase shift from $\pi/2$ corresponds to the maximum value of i_b (TSC current) as can be seen from Eqs. [10] and [14]. The position of T_m for well-poled samples prepared at room temperature depends on the rest time, t_r, through the phenomenological relationship $T_m = 309 + 6.5 \log(t_r)$ which has been extracted from the data of Ref. (18). For samples rested three days, t_r = 72 hours, T_m corresponds to $\sim$47°C as indicated in the phase-shift data of Fig. 5. The absolute value of the phase angle is dependent upon the temperature-wave-period as seen from Eq. [10] and is also in evidence in Fig. 5.

Second and subsequent thermal cycles yield $\pi/2$ phase shifts for these same samples indicating reversible and reproducible pyroelectric behavior. Figure 6 shows a plot of the computed and measured phase

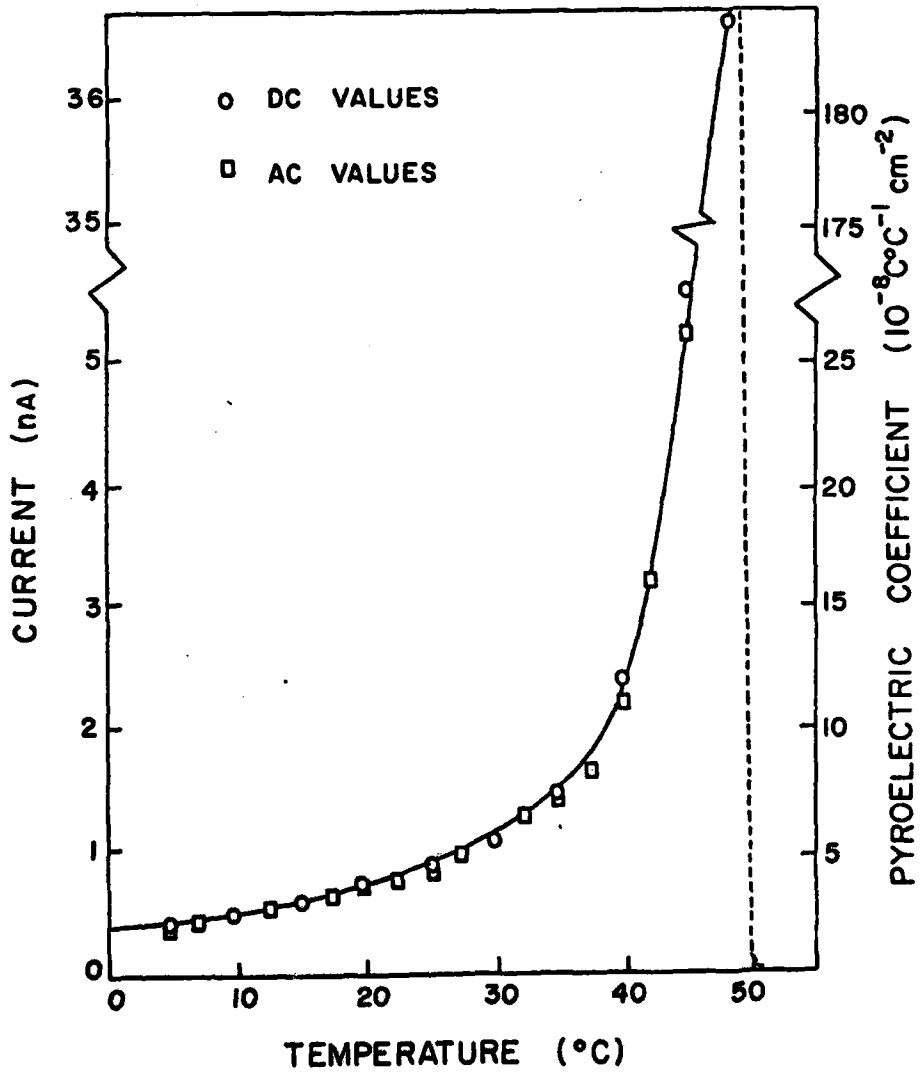

Figure 3. Measured ac and dc-pyroelectric current and corresponding pyroelectric coefficients for triglycine sulfate for a 20-second temperature wave period.

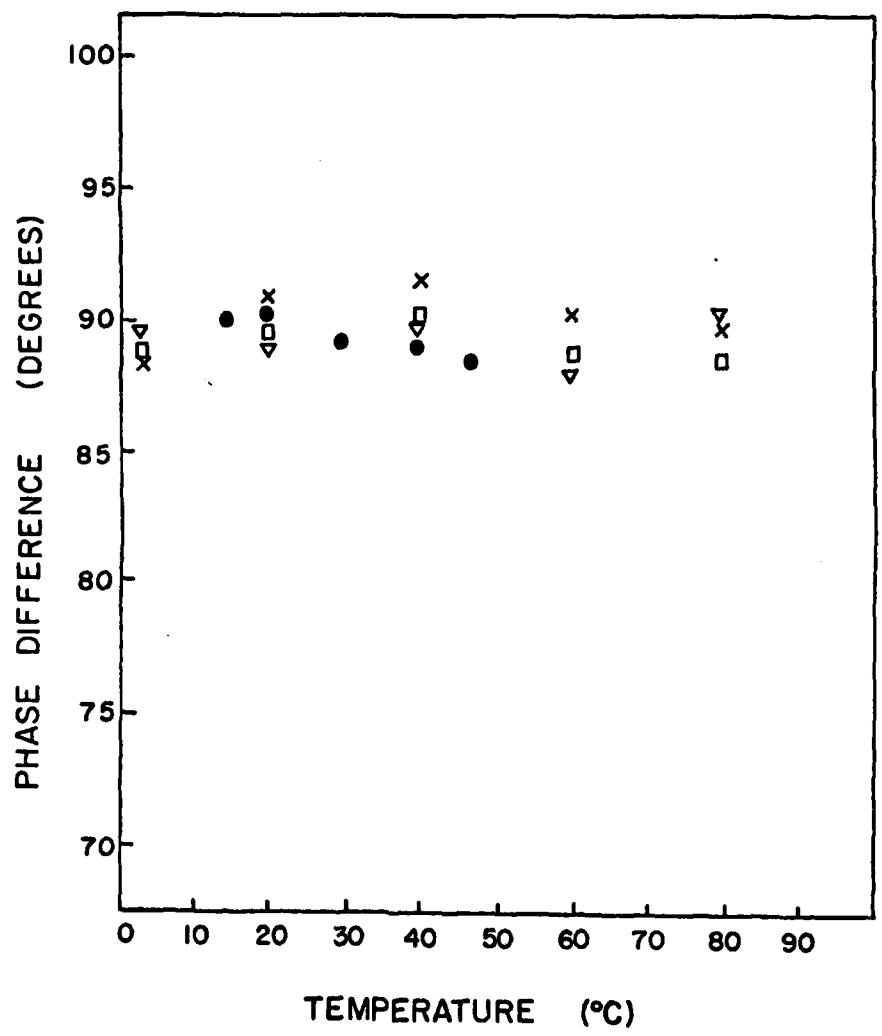

Figure 4. Phase difference between measured current and applied ac-temperature wave as a function of temperature for TGS (20 sec-●) and $LiTaO_3$ (5 sec-X), (50 sec-□), and (200 sec-Δ).

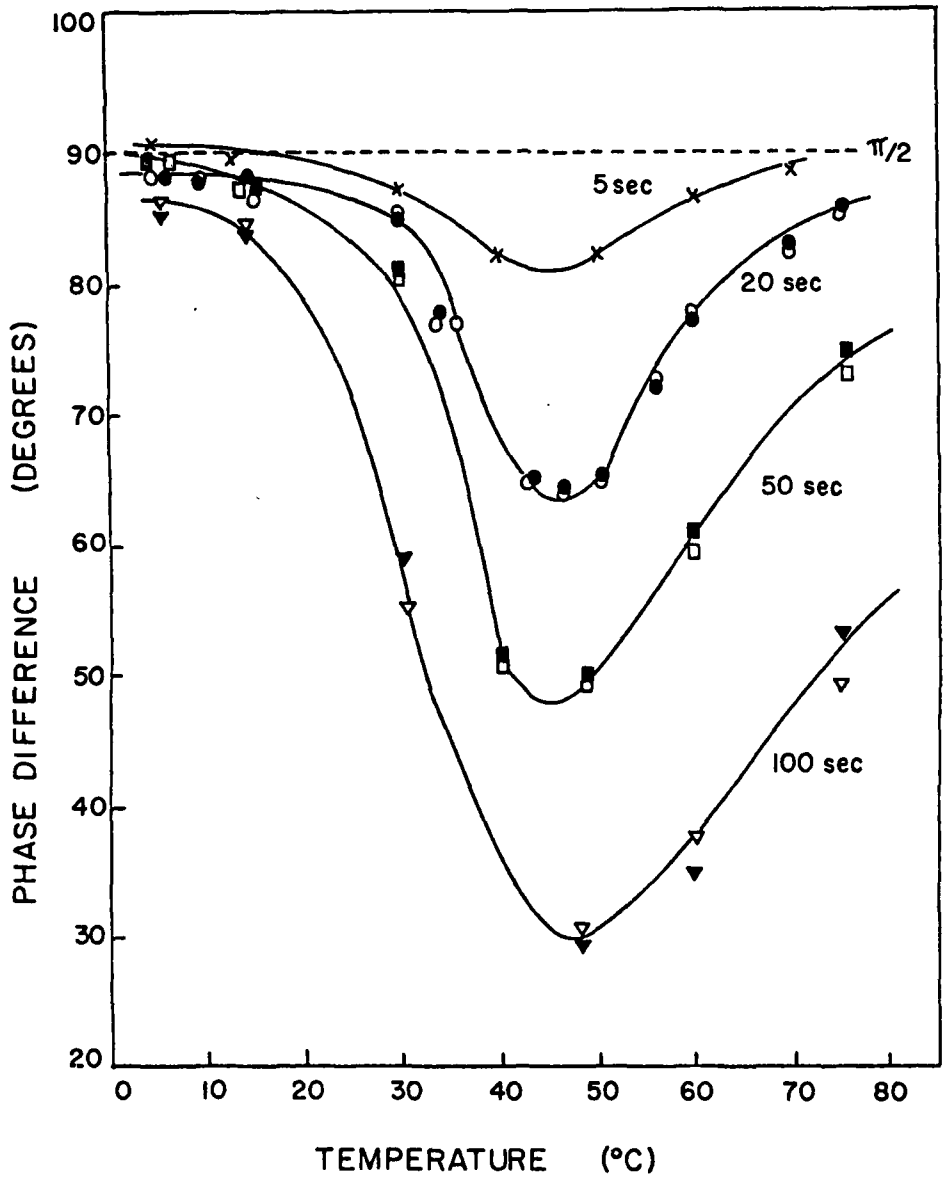

Figure 5. First thermal cycle phase difference between measured current and ac-temperature waves as a function of temperature for identically poled PVF_2 samples. Here solid points are computed from Eq. [10] and the open points are determined graphically from the data.

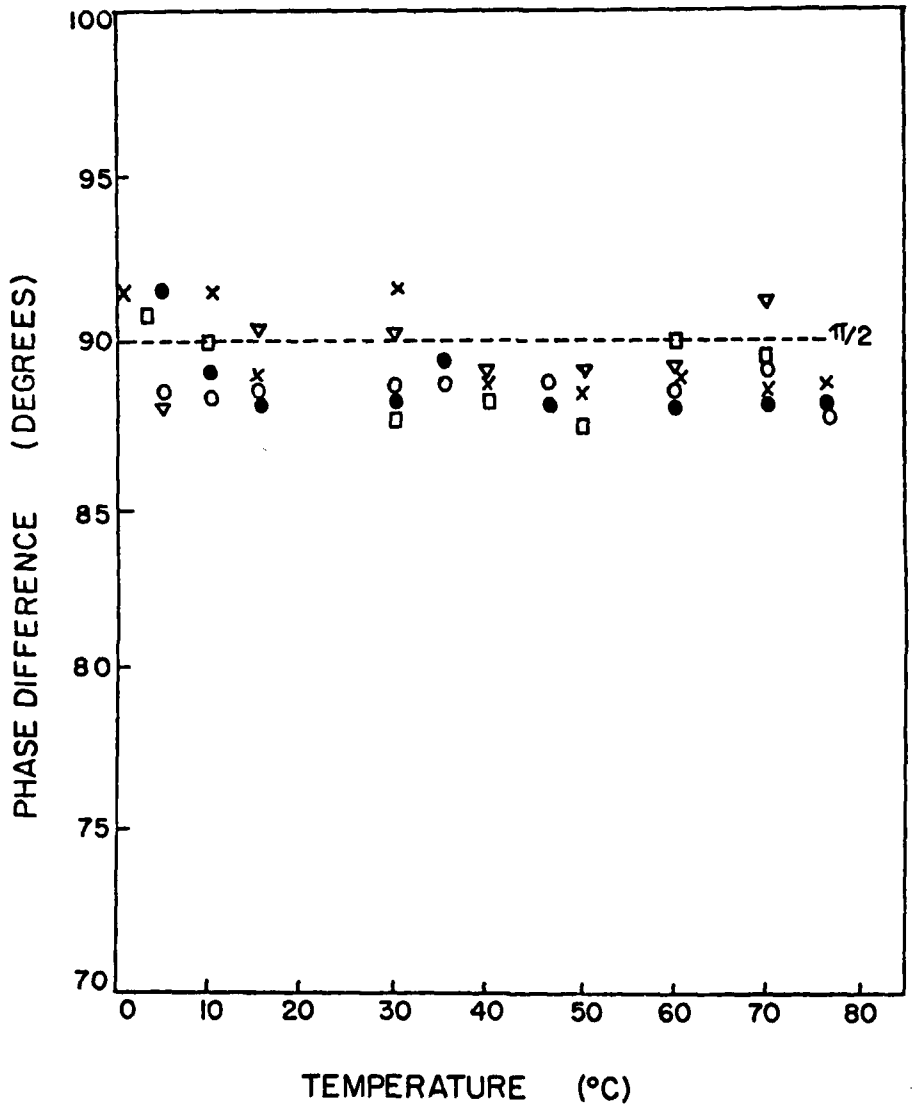

Figure 6. Computed (solid points) and measured (open points) phase differences of the second and third thermal cycles for identically poled PVF_2 samples. Here (20 sec-X), third run; (20 sec-○), (5 sec-△), and (50 sec-□), all second run; and (20 sec-●), computed second run.

shifts of the second and third thermal cycles for temperature wave periods of 5, 20, and 50 seconds.

CONCLUSIONS

A method has been described which allows one to analyze complicated currents emanating from warmed dielectrics. This technique is easily applied for temperature waves of certain amplitude and frequency limits and permits an accurate assessment of dielectric materials being examined for specific applications, such as infrared detectors or vidicon targets, where it is necessary to know the current magnitude and relaxation properties as a function of temperature and temperature changes.

The low-frequency temperature wave method is a direct dynamic measurement of the pyroelectric coefficient. This method eliminates the need for measurements of specific heats, dielectric constants, and radiation absorption coefficients as well as identifying the effects due to irreversible currents which occur when samples are heated at a constant rate.

REFERENCES

1. Nakamura, K. and Wada, Y., J. Polym. Sci. A29:161 (1971).
2. Bergman, J. G. Jr., McFee, J. H., and Crane, G. R., Appl. Phys. Letters, 18:203 (1971); McFee, J.H., Bergman, J. G. Jr., and Crane, G.R., Ferroelectrics, 3: 305 (1972).
3. Blevin, R. W. and Geist, J., Appl. Opt., 13:2212 (1974).
4. Bergman, J. G. Jr., Crane, G. R., Ballman, A. A., and O'Bryan, H. M. Jr., Appl. Phys. Letters, 21:497 (1972).
5. Glass, A. M., McFee, J. H., Bergman, J. G. Jr., J. Appl. Phys., 42:5219 (1971).
6. Peterson, R. L., Day, G. W., Gruzensky, P. M., and Phelan, R. J. Jr., J. Appl. Phys., 45:3296 (1974).
7. Stephens, A. W., Levine, A. W., Fech, J. Jr., Zrebiec, T. J., Cafiero, A. V., and Garofalo, A. M., Thin Solid Films, 20:361 (1974).
8. Garn, L. E., and Sharp, E. J., IEEE Trans. Parts, Hybrids, Packag., PHP-10:208 (1974).
9. Stern, J. and Edleman, S., Tech. News Bull. NBS, 56:52 (1972).
10. Wada, Y., and Hayakawa, R., Japan J. Appl. Phys., 15:2041 (1976).
11. Das-Gupta, D. K., and Duffy, J. S., J. Appl. Phys., 50:561 (1979).
12. Chynoweth, A. G., J. Appl. Phys., 27:78 (1956).
13. Glass, A. M., J. Appl. Phys., 40:4699 (1969).
14. Byer, R. L., and Roundy, C. B., IEEE Trans. Sonics Ultrason., SU-19:333 (1972).

15. Creswell, R. A., Perlman, M. M., and Kabayama, M. A., in Dielectric Properties of Polymers, edited by Karasz, F. E., (Plenum, New York, 1972), p. 295ff.
16. Das-Gupta, D. K., Ferroelectrics, 33:75 (1981).
17. Burkhard, H., and Pfister, G., J. Appl. Phys., 45:3360 (1974).
18. Sharp, E. J., and Garn, L. E., Appl. Phys. Letters, 29:480 (1976).
19. Garn, L. E., Dissertation, American Univ., (1977).
20. Garn, L. E., and Sharp, E. J., (submitted to J. Appl. Phys.).
21. Creswell, R. A., and Perlman, M. M., J. Appl. Phys., 41:2365 (1970).
22. Perlman, M. M., J. Appl. Phys., 42:2645 (1971).
23. Glass, A. M., Phys. Rev., 172:564 (1968).
24. Lines, M. E., and Glass, A. M., Phys. Rev. Letters, 39:1362 (1977).
25. Glass, A. M., Appl. Phys. Letters, 13:147 (1968).
26. Taylor, R. G. F., and Boot, H. A. H., Contemp. Phys., 14:55 (1973).
27. Day, G. W., Hamilton, C. A., Peterson, R. L., Phelan, R. J. Jr., and Mullen, L. O., Appl. Phys. Letters, 24:456 (1974).
28. Das-Gupta, D. K., and Doughty, K., J. Appl. Phys., 49:4601 (1978); IEEE, Trans. Industry Appl., IA-14:448 (1978); J. Appl. Phys., 51:1733 (1979).